



## Phosphodiesterase inhibitors. Part 4: Design, synthesis and structure-activity relationships of dual PDE3/4-inhibitory fused bicyclic heteroaromatic-4,4-dimethylpyrazolones

Koji Ochiai<sup>a</sup>, Satoshi Takita<sup>a</sup>, Akihiko Kojima<sup>a</sup>, Tomohiko Eiraku<sup>a</sup>, Naoki Ando<sup>a</sup>, Kazuhiko Iwase<sup>a</sup>, Tetsuya Kishi<sup>a</sup>, Akira Ohinata<sup>a</sup>, Yuichi Yageta<sup>a</sup>, Tokutaro Yasue<sup>a</sup>, David R. Adams<sup>b</sup>, Yasushi Kohno<sup>a,\*</sup>

<sup>a</sup> Discovery Research Laboratories, Kyorin Pharmaceutical Co., Ltd., 2399-1, Nogi, Nogi-machi, Shimotsuga-gun, Tochigi 329-0114, Japan

<sup>b</sup> Chemistry Department, School of Engineering and Physical Sciences, Heriot-Watt University, Riccarton, Edinburgh EH14 4AS, UK

### ARTICLE INFO

#### Article history:

Received 7 June 2012

Revised 11 July 2012

Accepted 24 July 2012

Available online 31 July 2012

#### Keywords:

Dual PDE3/4 inhibitor  
Pyrazolo[1,5-*a*]pyridine  
Dimethylpyrazolone  
Asthma  
COPD

### ABSTRACT

(-)-6-(7-Methoxy-2-trifluoromethylpyrazolo[1,5-*a*]pyridin-4-yl)-5-methyl-4,5-dihydro-3-(2*H*)-pyridazinone (KCA-1490) is a dual PDE3/4 inhibitor that exhibits potent combined bronchodilatory and anti-inflammatory activity. Here we show that a 4,4-dimethylpyrazolone subunit serves as an effective surrogate for the 5-methyl-4,5-dihydropyridazin-3(2*H*)-one ring of KCA-1490 whilst lacking a stereogenic centre. The 2- and 7-substituents in the pyrazolo[1,5-*a*]pyridine subunit markedly influence the PDE-inhibitory profile and can be adjusted to afford either potent PDE4-selective inhibitors or dual PDE3/4 inhibitors. A survey of bicyclic heteroaromatic replacements for the pyrazolo[1,5-*a*]pyridine allowed further refinement of the inhibitory profile and identified 3-(8-methoxy-2-(trifluoromethyl)imidazo[1,2-*a*]pyridin-5-yl)-4,4-dimethyl-1*H*-pyrazol-5(4*H*)-one as an orally active, achiral KCA-1490 analog with well-balanced dual PDE3/4-inhibitory activity.

© 2012 Elsevier Ltd. All rights reserved.

Cyclic 3',5'-nucleotide phosphodiesterase (PDE) enzymes mediate the hydrolytic degradation of key second messengers, cyclic adenosine monophosphate (cAMP) and cyclic guanosine monophosphate (cGMP), to their respective parent nucleoside 5'-monophosphates (AMP and GMP). There are 11 PDE gene families and, of these, the PDE4 family in particular plays a pivotal role in regulating a network of inflammatory mediators by controlling intracellular levels and gradients of cAMP.<sup>1</sup> Interest in PDE4 as a therapeutic target stems, in part, from the pronounced anti-inflammatory activity exhibited by PDE4 inhibitors, with efforts to harness this activity recently culminating in the launch of roflumilast for treatment of severe chronic obstructive pulmonary disease (COPD).<sup>2</sup> The efficacy of PDE4 inhibitors for treatment of respiratory disease may be augmented by a capacity to induce relaxation of airway smooth muscle, although inhibition of PDE3 is more effective in this regard.<sup>3</sup> For this reason we have been exploring the potential of dual PDE3/4 inhibitors as the basis for a new approach to treating asthma and COPD, and have previously identified fused bicyclic heteroaromatic-dihydropyridazinones, typified by KCA-1490 (Fig. 1), as dual PDE3/4 inhibitors that exhibit promising activity in pharmacological models of inflammation

and bronchoconstriction.<sup>4,5</sup> Although the individual PDE3- and PDE4-inhibitory components of KCA-1490 are modest, we attribute the potent combined anti-inflammatory and bronchodilatory activity of this compound and its analogs to their balanced dual PDE3/4-inhibitory profile, where the combination of PDE3 and PDE4 inhibition is thought to function additively or synergistically to induce airway smooth muscle relaxation.<sup>6</sup>

In developing KCA-1490, we combined the pyrazolo[1,5-*a*]pyridine core of our LTD4-antagonist and nonselective PDE inhibitor, ibudilast (Fig. 1),<sup>7</sup> with a 5-methyl-4,5-dihydropyridazin-3(2*H*)-one subunit. The latter was originally introduced because the dihydropyridazinone ring is a common structural component of established PDE3 inhibitors such as imazodan<sup>8</sup> and CI-930.<sup>9</sup> Our preliminary work revealed that replacement of the pyridazinone ring of KCA-1490 with closely related subunits, for example 5,5-dimethyl-4,5-dihydropyridazin-3(2*H*)-one and 5-methylpyridazin-3(2*H*)-one, resulted in a loss of both PDE3 and PDE4 inhibitory activity. The 5-methyl-4,5-dihydropyridazin-3(2*H*)-one was thus found to be the most effective pyridazinone-based substituent for the 4-position of the pyrazolo[1,5-*a*]pyridine core, albeit having the drawback of introducing chirality into the structure.<sup>4</sup>

In order to eliminate the stereogenic center of KCA-1490, we needed to identify alternative, achiral scaffolds that could replace the 5-methyl-4,5-dihydropyridazin-3(2*H*)-one subunit whilst maintaining the dual PDE3/4-inhibitory profile of the parent

\* Corresponding author.

E-mail address: [yasushi.kohno@mb.kyorin-pharm.co.jp](mailto:yasushi.kohno@mb.kyorin-pharm.co.jp) (Y. Kohno).

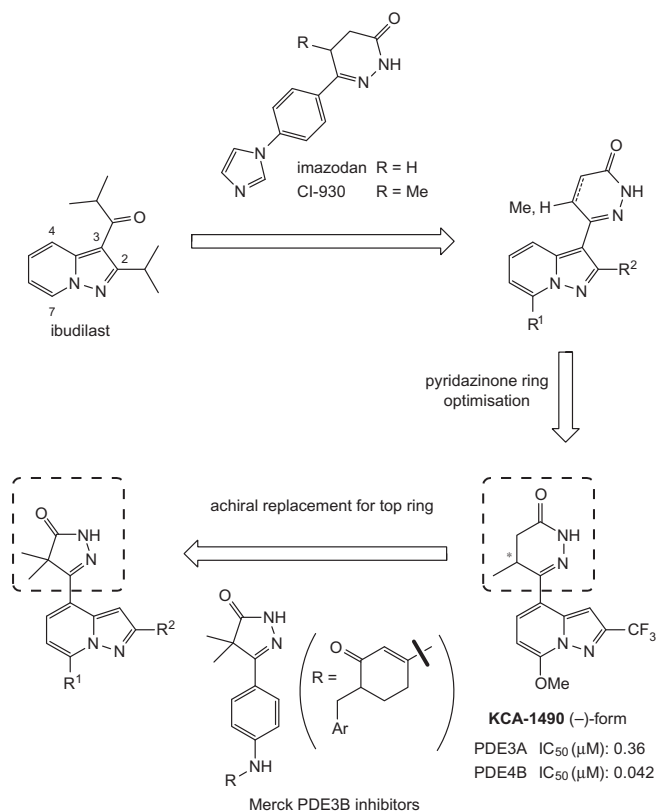


**Figure 1.** Discovery and development pathway for pyrazolopyridine-based dual PDE3/4 inhibitor, KCA-1490. Activity data quoted here for KCA-1490 are for inhibition of the isolated core catalytic domains of PDE3A and PDE4B.

compound. To this end we first chose to explore a 4,4-dimethylpyrazolone replacement for the pyridazinone ring of KCA-1490

because pyrazolones are well established as ring contracted mimics of dihydropyridazinone PDE3 inhibitors.<sup>10</sup> Moreover, in recent years Merck have actively developed a series of 3-aryl-4,4-dimethyl-1*H*-pyrazol-5(4*H*)-one derivatives (Fig. 1) as potent and selective PDE3B inhibitors.<sup>11</sup> Here, we describe a novel series of 4,4-dimethylpyrazolone dual PDE3/4 inhibitors derived from KCA-1490. A survey of potential bicyclic heteroaromatic replacement subunits for the pyrazolo[1,5-*a*]pyridine core of this series has also been undertaken and the activity of the resulting compounds is disclosed.

Our general synthetic route to the pyrazolopyridine–pyrazolone target compounds is summarized in Scheme 1 (see Supplementary data).<sup>12</sup> In brief, treatment of pyridine derivatives **1** with *O*-mesitylenesulfonylhydroxylamine (MSH) in CH<sub>2</sub>Cl<sub>2</sub> gave *N*-aminopyridinium salts **2**. The pyrazolo[1,5-*a*]pyridine ring was constructed by the reaction between **2** and appropriate alkynes under basic conditions to afford **3**. Synthesis of ketones **4** from **3** was performed by three methods. For routes commencing with 3-methoxy pyridine starting materials (**1**, R<sup>1</sup> = OMe), the sequence used for conversion of **3** into **4** comprised demethylation of the 4-methoxy group, decarboxylation or deacylation at the 3-position, triflate derivatisation of the resulting 4-hydroxypyrazolo[1,5-*a*]pyridine and finally Heck reaction with *n*-butyl vinyl ether (Method A). For pyrazolopyridine intermediates (**3**; R<sup>1</sup> = CH<sub>2</sub>OH; R<sup>4</sup> = OMe, OEt, OBn), synthesis of **4** was accomplished in a 5-step sequence consisting of ester hydrolysis, decarboxylation, MnO<sub>2</sub> oxidation, and Grignard reaction followed by Parikh–Doering oxidation or Swern oxidation. In cases where a ketone moiety was preinstalled in pyridines **1**, intermediates **4** were obtained by decarboxylation or deacylation to remove the pyrazolopyridine 3-substituent in **3** (Method C). Construction of the 4,4-dimethylpyrazolone ring was achieved by first converting ketones **4** into pyrazolone precursors **5** through a 2-step sequence beginning with introduction of a methoxycarbonyl group and

**Table 1**

SAR survey for optimization of the pyrazolopyridine 7-substituent

Cmpd	R	Inhibition IC <sub>50</sub> (μM) <sup>a</sup>	
		PDE3A	PDE4B
<b>7<sup>b</sup></b>		11.3	0.47
<b>6a</b>	Me	2.37	0.16
<b>6b</b>	Et	2.00	0.017
<b>6c</b>	OMe	9.21	0.41
<b>6d</b>	SMe	9.01	0.079
<b>6e</b>	NHMe	75.55	0.015
<b>6f</b>	CH <sub>2</sub> OH	1.59	0.035
<b>6g<sup>c</sup></b>	CH(OH)Me	1.63	0.0034
<b>6h</b>	Ac	2.50	0.0075

**Scheme 1.** Reagents and conditions: (a) MSH / DCM, rt; (b) R<sup>3</sup>-C≡C-COR<sup>4</sup>, K<sub>2</sub>CO<sub>3</sub> / EtOH, rt; (c) (**Method A**: R<sup>1</sup> = OMe): (i) 48% HBr aq reflux or BBr<sub>3</sub> / DCM, 0 °C then 50% H<sub>2</sub>SO<sub>4</sub> aq, 150 °C, (ii) Tf<sub>2</sub>O, Et<sub>3</sub>N / DCM, 0 °C, (iii) *n*-butyl vinyl ether, Pd(OAc)<sub>2</sub>, DPPP, Et<sub>3</sub>N / DMF, 80 °C. (**Method B**: R<sup>1</sup> = hydroxymethyl): (i) KOH aq. / EtOH, reflux, (ii) PhCH<sub>3</sub>, reflux, (iii) MnO<sub>2</sub> / CHCl<sub>3</sub>, 50 °C, (iv) EtMgBr / THF, 0 °C to rt, (v) SO<sub>3</sub>-pyridine, Et<sub>3</sub>N / DMSO, rt or TFAA, DMSO / DCM, -78 °C then Et<sub>3</sub>N, -78 °C to rt. (**Method C**: R<sup>1</sup> = acetyl, propionyl) 48% HBr aq, reflux or 50% H<sub>2</sub>SO<sub>4</sub> aq, 150 °C or (i) KOH aq / EtOH, reflux, (ii) PhCH<sub>3</sub>, reflux; (d) (i) NaH, dimethyl carbonate, reflux, (ii) NaH, MeI / DMF, rt; (e) hydrazine, AcOH / EtOH, reflux or *t*-butyl carbazate, PPTS / xylene, reflux.

<sup>a</sup> Enzyme assays were performed using the core catalytic domains from the PDE3A and PDE4B isoforms according to previously procedures.<sup>7b</sup> Data reported are the mean of at least three experiments.

<sup>b</sup> 6-(2-Ethyl-7-methoxy-pyrazolo[1,5-*a*]pyridin-4-yl)-5-methyl-4,5-dihydro-3-(2*H*)-pyridazinone (racemic form).<sup>4</sup>

<sup>c</sup> **6g** was tested in racemic form.

followed by methylation (for **4**,  $R^5 = \text{Et}$ ) or dimethylation (for **4**,  $R^5 = \text{Me}$ ) at the  $\alpha$ -position next to the carbonyl group. Closure of the pyrazolone ring was then accomplished by the reaction of **5** with hydrazine to afford the target compounds (**6**). In the case of the 7-methoxy-2-trifluoromethyl derivative, *t*-butyl carbazate was employed instead of hydrazine because the high nucleophilicity of hydrazine resulted in an undesired side reaction at the pyrazolopyridine 2-position.<sup>13</sup> For a number of the analogs introduction of the pyrazolopyridine 7-substituent was accomplished after initial formation of the core bicyclic. This was typically achieved by acetal protection of the ketone in **4** followed by lithiation, iodination, deprotection of the acetal and iodide substitution with an appropriate nucleophile (e.g., methoxide, methanethiolate, methylamine). A similar lithiation strategy followed by formylation (using ethyl formate) was used to develop some of the carbon-based substituents at the pyrazolopyridine 7-position. (Full details are presented in the Supplementary data).

Our foundational studies leading to KCA-1490 had revealed key roles for the pyrazolopyridine 2- and 7-substituents in shaping the PDE3/4-inhibitory profile of the compounds.<sup>4</sup> We therefore undertook a focused structure activity relationship (SAR) survey for substituents at these positions in our pyrazolone series. To explore the impact of substituents at the 7-position of the pyrazolo[1,5-*a*]pyridine (Table 1) we selected ethyl as the invariant group at C-2 in order to make a direct comparison with the activity of the corresponding pyridazinone analogs in our previously published work leading to KCA-1490.<sup>4</sup> For this purpose, compounds were assayed for inhibitory activity against the core catalytic domains from PDE3A and PDE4B using previously reported protocols.<sup>7b,14</sup>

All compounds other than the 7-NHMe derivative (**6e**) exhibited comparable levels of PDE3 inhibition to the corresponding pyridazinone derivatives in the KCA-1490 series.<sup>4</sup> Surprisingly, **6e** showed very weak PDE3 inhibitory activity. In contrast the activity of the 7-OMe derivative (**6c**) was essentially the same as the corresponding pyridazinone (**7**, included in Table 1 for reference). SAR analysis of our own pyridazinone series,<sup>4,5,15</sup> corroborated by the protein cocrystal structure for a PDE3-selective 5-methyl-4,5-dihydropyridazinone inhibitor from Merck,<sup>16</sup> have implicated a binding mode in which the pyridazinone ring docks to a region of the substrate-binding pocket distal to the catalytic metal centers, engaging the conserved purine-scanning glutamine (a residue that hydrogen bonds the cAMP adenine during catalytic turnover). It is likely that this mode of interaction, illustrated in Figure 2 A for

compound **6f**, is conserved in the pyrazolone series, because a favorable supplementary hydrogen bond from the pyrazolone carbonyl group to a distal histidine residue may also be formed (Fig. 2A). However, pyridazinone ring contraction will have an important impact on the position occupied by the connected pyrazolopyridine subunit. In particular, fitting the pyrazolone series compounds to this model positions the pyrazolopyridine core more deeply within the catalytic pocket, close to the proximal histidine (a residue adjacent to the metal centers that is conserved across all PDEs and that functions as a proton donor during substrate hydrolysis). Our analysis of this binding mode suggests that unfavorable steric compression will arise in the case of 7-substituents that adopt a conformation coplanar with the pyrazolopyridine. Indeed loosening of the hydrogen bonds that anchor the pyrazolone ring in the distal region of the pocket may be necessary to accommodate such groups on the inhibitor. We therefore propose that the weak PDE3-inhibitory activity for 7-NHMe derivative (**6e**) in the pyrazolone series may be due to a particularly strong bias for such a conformation with the methylamino group. In contrast, heteroatom-linked groups of similar size (**6c**, 7-OMe; **6d**, SMe) that have a less pronounced preference for coplanarity with the pyrazolopyridine are expected to be more readily accommodated, as are carbon based substituents linked through an  $\text{sp}^3$  centre [**6b**, 7-Et; **6f**, 7- $\text{CH}_2\text{OH}$ ; **6f**, 7- $\text{CH}(\text{Me})\text{OH}$ ] or an  $\text{sp}^2$  centre (**6h**, 7-Ac), but where a degree of twist on the connecting bond to the pyrazolopyridine is likely.

SAR analysis in our foundational pyridazinone compound series,<sup>4,5,15</sup> has suggested a PDE4-binding mode that differs profoundly from that invoked for PDE3. As illustrated in Figure 2B for compound **6f**, it is proposed that the bound orientation of the inhibitor is reversed so that the pyrazolopyridine engages the purine-scanning glutamine. In the case of 7-methoxy pyrazolopyridines, such as KCA-1490 and its ethyl analogue (**7**), both the pyrazolopyridine N(1) center and the methoxy group are expected to hydrogen bond to the purine scanning glutamine in a manner that is very well established from PDE4 X-ray co-crystal structures with catechol ethers such as roflumilast.<sup>14b,18</sup> Such a binding mode would position the 7-OMe group within the confined PDE4 Q<sub>1</sub> subpocket, as defined by Card et al.,<sup>18</sup> with the pyrazolopyridine 2-substituent directed into the Q<sub>2</sub> subpocket (labelled in Fig. 2B) at the opening of catalytic pocket and adjacent to the purine-scanning glutamine. The 7-OMe derivative (**6c**) in the pyrazolone series was essentially identical in its PDE4-inhibitory activity to the

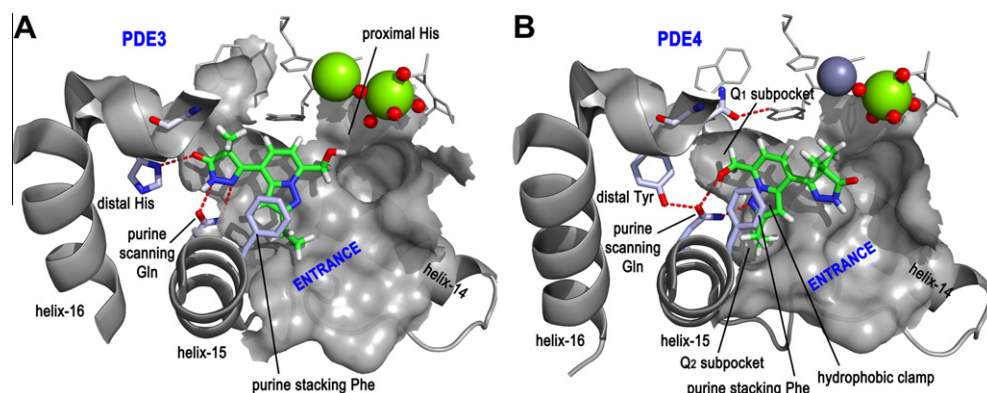


**Figure 2.** Interaction models for compound **6f** (green stick) with PDE3 (panel A) and PDE4 (panel B). The PDE3-binding model is templated on the co-crystal structure (PDB: 1SO2) of (*R*)-6-(4-([2-(3-iodobenzyl)-3-oxocyclohex-1-en-1-yl]amino)phenyl)-5-methyl-4,5-dihydropyridazin-3(2*H*)-one with the core catalytic domain from PDE3B.<sup>16</sup> Residues lining the catalytic pocket of PDE3B are fully conserved in the core catalytic domain of PDE3A (used in the enzyme inhibition assays of the present study). In this binding pose the pyrazolone ring hydrogen bonds (dotted lines) the PDE3 purine-scanning Gln and His residues distal to the catalytic metal centers (large spheres). The PDE4 binding model is templated on the co-crystal structure of zardaverine with the core catalytic domain of PDE4D (PDB: 1XOR, 1MKD).<sup>17</sup> Residues lining the catalytic pocket are fully conserved between PDE4D and PDE4B (the latter used in the assays of the present study). The profound difference in orientation of bound inhibitor between the two models is a consequence of differences between PDE3 and PDE4 in residues lining the distal region of the catalytic pocket. The Q<sub>1</sub> subpocket in PDE4 is more restricted and lacks the hydrogen bonding feature afforded by the distal His residue in PDE3.

corresponding analog (**7**) in the pyridazinone series, and it is probable that both compounds adopt this catechol ether-like binding mode.

Interestingly the 7-Et derivative (**6b**) was some 25-fold more effective as a PDE4 inhibitor than the 7-OMe analog (**6c**), revealing that strict catechol ether mimicry is not required and indeed potentially detrimental to PDE4-inhibitory activity. In the case of **6c** it is likely that slight adjustment in the orientation of the pyrazolopyridine allows geometrical optimization of a single, strong hydrogen bond between the pyrazolopyridine N(1) center and the purine-scanning glutamine NH<sub>2</sub> whilst simultaneously positioning the 7-Et group more favorably in the Q<sub>1</sub> subpocket. Potentially, the 7-SMe derivative (**6d**) might be rather similar in that regard. The 10-fold enhancement in activity of the 7-Et analog (**6b**) compared to the 7-Me analog (**6a**) suggests that optimal occupancy of the Q<sub>1</sub> subpocket is particularly important for achieving potent PDE4 inhibition. We did not examine the activity of the 7-Et analog in the pyridazinone series.<sup>4</sup> However, the 7-Me derivative in that series exhibited similar PDE3- and PDE4-inhibitory activity to the cognate compound (**6b**) presented in Table 1.

Our PDE3-binding model for compounds **6a–6h** does not invoke a hydrogen bonding interaction between the protein and functional groups at the pyrazolopyridine 7-position. This is consistent with the rather narrow PDE3-inhibitory activity range observed across this compound set (with the exception of **6e**, discussed above). In contrast, hydrogen bonding features in the pyrazolopyridine 7-substituent profoundly influence the PDE4-inhibitory activity of the compounds. Moreover, the activity data in Table 1 suggest that appropriate hydrogen donor or acceptor features may both support potent PDE4-inhibitory activity, and some variation in the hydrogen bonding pattern between protein and ligand is conceivable. Thus, with the 7-acetyl derivative (**6h**) the pyrazolopyridine N(1) center and carbonyl oxygen may deliver a pincer-like engagement of the glutamine NH<sub>2</sub> whilst positioning the acetyl methyl group effectively in the Q<sub>1</sub> subpocket. On the other hand, with the 7-hydroxymethyl derivative (**6f**) the side chain hydroxy group may target the glutamine O(ε) centre, as illustrated (Fig. 2B). Interestingly a branched methyl extension of the hydroxymethyl side chain in **6f** (to give **6g**) affords a 10-fold enhancement in PDE4-inhibitory potency, similar to the enhancement seen with the chain extension from methyl to ethyl (**6a** to **6b**). The particularly potent PDE4-inhibitory activity of **6g**, which was assessed in racemic form, probably arises therefore from a combination of optimal hydrogen bonding to the purine-scanning glutamine and fit of the 1-hydroxyethyl group within the Q<sub>1</sub>

subpocket. Given the confines of that site, a difference in activity between the two enantiomers of **6g** is clearly to be expected. We have not, however, assessed the two enantiomers separately to determine the extent to which the activity resides with one or the other.

The data summarised in Table 1 highlight the importance of the pyrazolopyridine 7-substituent in controlling the levels of PDE4 inhibition exhibited by members of the compound series. Although our primary focus is the development of dual PDE3/4 inhibitors, the data demonstrate that appropriate selection of that substituent can deliver both very potent PDE4 inhibitors (**6g** and **6h**, IC<sub>50</sub> = 3.4 nM and 7.5 nM respectively) and switch the inhibitory profile from dual PDE3/4 inhibition to selective PDE4 inhibition (**6e**, IC<sub>50</sub> = 15 nM with 5000-fold selectivity over PDE3).

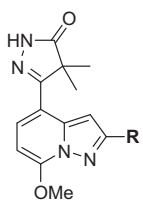
Our SAR survey of pyrazolopyridine 2-substituents (Table 2) was undertaken with methoxy as the invariant group in the 7-position. We opted for the methoxy group rather than substituents that confer more potent PDE4 inhibition because we had attributed the potent combined bronchodilatory and anti-inflammatory activity of KCA-1490 to its balanced dual PDE3/4-inhibitory profile. The activity balance of both the 7-OMe and 7-Me derivatives (**6c** and **6a** respectively, Table 1) was similar to KCA-1490.<sup>4</sup> However, in the pyridazinone series the 7-Me analog failed to show activity *in vivo*, thus dictating our selection of the 7-OMe group for the pyrazolone series SAR survey presented here.<sup>4</sup> Guided by our work with the pyridazinones, we focused on a limited population of 2-substituents that we had previously found to show promise. All of these compounds (**6i–6l**) had similar levels of inhibitory activity against PDE3 (within a threefold range) and were less potent than the cognate pyridazinone analogs including KCA-1490.<sup>4</sup> The consistently weaker PDE3-inhibitory activity in this pyrazolone series likely reflects changes in the enzyme-bound position and orientation of the pyrazolopyridine subunit associated with the ring contraction (*vide supra*).

A notable feature in the PDE4-inhibitory activity of the Table 2 compound set was the pronounced loss of activity for the 2-H derivative (**6i**). A similar activity loss was observed in the pyridazinone series,<sup>4</sup> and this highlights the importance of a suitably sized substituent targeted to the Q<sub>2</sub> subpocket for conferring effective PDE4 inhibition. Although the 2-CHF<sub>2</sub> and 2-CF<sub>3</sub> compounds (**6k** and **6l**) possessed comparable levels of PDE4 inhibition to KCA-1490, neither compound was as effective in inhibiting PDE3. This prompted us to explore replacement fused bicyclic heteroaromatic subunits for the pyrazolopyridine.

We had previously evaluated<sup>5</sup> a set of pyrazolopyridine replacement subunits in the pyridazinone series derived from KCA-1490 and found that both PDE3- and PDE4-inhibitory performance could be modestly improved by optimization of interactions within the ‘hydrophobic clamp’<sup>19</sup> of the catalytic pocket, a feature provided by the purine-stacking phenylalanine residue and the surface of helix-14 (marked in Fig. 2). We therefore decided to evaluate a similar set of analogs in the pyrazolone series (Table 3) and selected CF<sub>3</sub> (or Et) and OMe as groups corresponding, respectively, to the 2- and 7-substituents of the pyrazolopyridine, as this combination had delivered promising compounds in the pyridazinone series. Synthesis of the required compound set (**6m–6s**) was undertaken by adaptation of the routes developed for the pyridazinone series (see Supplementary data).<sup>5,20</sup>

In the case of PDE3 a likely alteration in the bound position of the heterobicycle allied to pyridazinone ring contraction (*vide supra*) made it difficult to predict whether PDE3-inhibitory activity in the pyrazolone series would parallel that in the pyridazinone series, where 4-methoxy-2-(trifluoromethyl)benzo[d]thiazol-7-yl and 8-methoxy-2-(trifluoromethyl)quinolin-5-yl analogs had performed better than the parent pyrazolopyridine whilst the 4-methoxy-2-(trifluoromethyl)-1*H*-benzo[d]imidazol-7-yl and

**Table 2**  
SAR survey for optimization of the pyrazolopyridine 2-substituent



Cmpd	R	Inhibition IC <sub>50</sub> (μM) <sup>a</sup>	
		PDE3	PDE4
KCA-1490		0.36	0.042
<b>6c</b>	Et	9.21	0.41
<b>6i</b>	H	10.84	2.93
<b>6j</b>	<i>c</i> -Pr	6.17	0.15
<b>6k</b>	CHF <sub>2</sub>	3.28	0.05
<b>6l</b>	CF <sub>3</sub>	4.13	0.11

<sup>a</sup> See footnotes to Table 1.

**Table 3**  
SAR survey for optimization of the fused bicyclic heteroaromatics

Cmpd	R	Inhibition IC <sub>50</sub> (μM) <sup>a</sup>		Cmpd	R	Inhibition IC <sub>50</sub> (μM) <sup>a</sup>	
		PDE3A	PDE4B			PDE3A	PDE4B
<b>KCA-1490</b>		0.36	0.042	<b>6o</b>		0.54	0.063
<b>6a</b>		9.21	0.41	<b>6p</b>		14.12	0.2
<b>6l</b>		4.13	0.11	<b>6q</b>		0.14	0.15
<b>6m</b>		1.1	0.36	<b>6r</b>		10.08	2.58
<b>6n</b>		5.36	0.69	<b>6s</b>		6.65	1.07

<sup>a</sup> See footnotes to Table 1.

7-methoxy-2-(trifluoromethyl)benzofuran-4-yl counterparts had performed approximately 10-fold less well. With the pyrazolones, Table 3, significant PDE3-inhibitory activity enhancement was seen with benzothiazole **6o** and benzimidazole **6p** did prove to be the weakest inhibitor, although it was only 3.4-fold less potent than the parent pyrazolopyridine (**6l**). However, in other respects PDE3-inhibitory activity trends between the two compound series broke down. Thus, in the pyrazolone series benzofuran **6m** showed a modest activity enhancement relative to pyrazolopyridine **6l** (instead of activity loss) and the imidazopyridine (**6q**) showed a striking 30-fold gain in inhibitory activity.

As with the pyridazinones, the PDE4-inhibitory activity of the benzothiazole analog (**6o**) in the pyrazolone series was also improved relative to the parent pyrazolopyridine (**6l**), albeit that the activity gain was modest. Other replacements for the pyrazolopyridine caused varying degrees of activity loss to a maximal 10-fold reduction in performance in the case of quinoline **6s**. The activity loss was marginal for imidazopyridine **6q**, however, and this resulted in a compound with almost equipotent inhibitory activity against PDE3 and PDE4 (IC<sub>50</sub> 150 nM).

Given the promising dual PDE3/4-inhibitory activity exhibited by benzothiazole **6o** and imidazopyridine **6q**, both compounds were further evaluated for their capacity to suppress histamine-induced bronchoconstriction in guinea pig according to an established procedure.<sup>21</sup> Testing was initially conducted with iv dosing at 0.3 mg/kg. As we expected, both **6o** and **6q** displayed potent bronchodilatory activity (96% and 100% suppression of bronchoconstriction vs control respectively). We next evaluated the bronchodilatory performance of **6o** and **6q** under po administration at

0.1 mg/kg in guinea pig. Unfortunately, benzothiazole derivative **6o** was not effective for suppression of histamine-induced bronchoconstriction under these conditions. This finding was consistent with our previous work in the pyridazinone series,<sup>4</sup> where the benzothiazole derivative was only weakly active under po administration, and is probably due to the vulnerability of the benzothiazole scaffold to metabolism under po administration.<sup>22</sup> On the other hand, imidazopyridine **6q** exhibited potent bronchodilatory potency under po administration (>70% inhibition of histamine-induced bronchoconstriction at 0.1 mg/kg).

In summary, we have demonstrated that an achiral 4,4-dimethylpyrazolone scaffold is an effective surrogate for the 5-methyl-4,5-dihydropyridazin-3(2H)-one subunit of our previously reported pyrazolopyridine-linked pyridazinone PDE inhibitors. Selection of an appropriate pyrazolopyridine 7-substituent can engender potent and, as in the case of 7-NHMe analog (**6e**), highly selective inhibitory activity against PDE4. However, the 4,4-dimethylpyrazolone also supports the development of well-balanced dual PDE3/4-inhibitory compounds, as with analog **6q**, where an isosteric imidazopyridine replacement was made for the pyrazolopyridine subunit of our original series. Imidazopyridine **6q** showed potent bronchodilatory activity under po administration with efficacy comparable to our chiral lead compound, KCA-1490.

#### Acknowledgments

We are grateful to Dr S. J. MacKenzie, Dr S. Hastings and Dr R. A. Clayton of the Kyorin Scotland Research Laboratory for their many valuable suggestions and performing the PDE inhibition assays.

## Supplementary data

Supplementary data associated with this article can be found in the online version, at <http://dx.doi.org/10.1016/j.bmcl.2012.07.088>.

## References and notes

- (a) Banner, K. H.; Moriggi, E.; Da Ros, B.; Schioppacassi, G.; Semeraro, C.; Page, C. P. *Br. J. Pharmacol.* **1996**, *119*, 1255; (b) Hatzelmann, A.; Schudt, C. *J. Pharmacol. Exp. Ther.* **2001**, *297*, 26.
- (a) Giembycz, M. A.; Field, S. K. *Drug Des. Dev. Ther.* **2010**, *4*, 147; (b) Lipworth, B. J. *Lancet* **2005**, *365*, 167; (c) Rabe, K. F.; Bateman, E. D.; O'Donnell, D.; Witte, S.; Bredenkroger, D.; Bethke, T. D. *Lancet* **2005**, *366*, 563.
- (a) Torphy, T. J.; Undem, B. J.; Cieslinski, L. B.; Luttmann, M. A.; Reeves, M. L.; Hay, D. W. *J. Pharmacol. Exp. Ther.* **1993**, *265*, 1213; (b) Bardin, P. G.; Dorward, M. A.; Lampe, F. C.; Franke, B.; Holgate, S. T. *Br. J. Clin. Pharmacol.* **1998**, *45*, 387; (c) Chung, K. F. *Eur. J. Pharmacol.* **2006**, *533*, 110.
- Ochiai, K.; Ando, N.; Iwase, K.; Kishi, T.; Fukuchi, K.; Ohinata, A.; Zushi, H.; Yasue, T.; Adams, D. R.; Kohno, Y. *Bioorg. Med. Chem. Lett.* **2011**, *21*, 5451.
- Ochiai, K.; Takita, S.; Eiraku, T.; Kojima, A.; Iwase, K.; Kishi, T.; Fukuchi, K.; Yasue, T.; Adams, D. R.; Allcock, R. W.; Jiang, Z.; Kohno, Y. *Bioorg. Med. Chem.* **2012**, *20*, 1644.
- (a) Torphy, T. J.; Burman, M.; Huang, L. B.; Tucker, S. S. *J. Pharmacol. Exp. Ther.* **1988**, *246*, 843; (b) de Boer, J.; Philpott, A. J.; van Amsterdam, R. G.; Shahid, M.; Zaagsma, J.; Nicholson, C. D. *Br. J. Pharmacol.* **1992**, *1028*, 106; (c) Torphy, T. J. *Am. J. Respir. Crit. Care Med.* **1998**, *157*, 351; (d) Underwood, D. C.; Bochnowicz, S.; Osborn, R. R.; Kotzer, C. J.; Luttmann, M. A.; Hay, D. W.; Gorycki, P. D.; Christensen, S. B.; Torphy, T. J. *J. Pharmacol. Exp. Ther.* **1998**, *287*, 988; (e) Schmidt, D. T.; Watson, N.; Dent, G.; Ruhlmann, E.; Branscheid, D.; Magnussen, H.; Rabe, K. F. *Br. J. Pharmacol.* **2000**, *131*, 1607; (f) Essayan, D. M. *Allergy J. Clin. Immunol.* **2001**, *108*, 671; (g) Boswell-Smith, V.; Spina, D.; Oxford, A. W.; Comer, M. B.; Seeds, E. A.; Page, C. P. *J. Pharmacol. Exp. Ther.* **2006**, *318*, 840.
- (a) Huang, Z.; Liu, S.; Zhang, L.; Salem, M.; Greig, G. M.; Chan, C. C.; Natsumeda, Y.; Noguchi, K. *Life Sci.* **2006**, *78*, 2663; (b) Gibson, L. C. D.; Hastings, S. F.; McPhee, I.; Clayton, R. A.; Darroch, C. E.; Mackenzie, A.; MacKenzie, F. L.; Nagasawa, M.; Stevens, P. A.; MacKenzie, S. J. *Eur. J. Pharmacol.* **2006**, *538*, 39.
- Sircar, I.; Duell, B. L.; Bobowski, G.; Bristol, J. A.; Evans, D. B. *J. Med. Chem.* **1985**, *28*, 1405.
- Bristol, J. A.; Sircar, I.; Moos, W. H.; Evans, D. B.; Weishaar, R. E. *J. Med. Chem.* **1984**, *1099*, 27.
- Sircar, I.; Morrison, G. C.; Burke, S. E.; Skeean, R.; Weishaar, R. E. *J. Med. Chem.* **1987**, *30*, 1724.
- Edmondson, S. D.; Mastracchio, A.; He, J.; Chung, C. C.; Forrest, M. J.; Hofsess, S.; MacIntyre, E.; Metzger, J.; O'Connor, N.; Patel, K.; Tong, X.; Tota, M. R.; Van der Ploeg, L.-H. T.; Varnerin, J. P.; Fisher, M. H.; Wyvratt, M. J.; Weber, A. E.; Parmee, E. R. *Bioorg. Med. Chem. Lett.* **2003**, *13*, 3983.
- Kohno, Y.; Ando, N.; Ochiai, K. Patent WO 2008129624; *PCT Int. Appl.*
- Ochiai, K.; Kojima, A.; Kohno, Y. *Chem. Pharm. Bull. (Tokyo)* **2012**, *60*, 267.
- (a) Houslay, M. D.; Adams, D. R. *Nat. Biotechnol.* **2010**, *28*, 38; (b) Burgin, A. B.; Magnusson, O. T.; Singh, J.; Witte, P.; Staker, B. L.; Bjornsson, J. M.; Thorsteinsdottir, M.; Hrafnisdottir, S.; Hagen, T.; Kiselyov, A. S.; Stewart, L. J.; Gurney, M. E. *Nat. Biotechnol.* **2010**, *28*, 63; (c) Day, J. P.; Lindsay, B.; Riddell, T.; Jiang, Z.; Allcock, R. W.; Abraham, A.; Sookup, S.; Christian, F.; Bogum, J.; Martin, E. K.; Rae, R. L.; Anthony, D.; Rosair, G. M.; Houslay, D. M.; Huston, E.; Baillie, G. S.; Klusmann, E.; Houslay, M. D.; Adams, D. R. *J. Med. Chem.* **2011**, *54*, 3331. We evaluated compound activity against the PDE core catalytic domains in our primary assays because sensitivity to inhibitors can be influenced by the nature and status of flanking regulatory regions in the enzymes, especially for the PDE4 family, where environment-dependent capping of the catalytic pocket catalytic by regulatory sequences may occur.
- Allcock, R. W.; Blakli, H.; Jiang, Z.; Johnston, K. A.; Morgan, K. M.; Rosair, G. M.; Iwase, K.; Kohno, Y.; Adams, D. R. *Bioorg. Med. Chem. Lett.* **2011**, *21*, 3307.
- Scapin, G.; Patel, S. B.; Chung, C.; Varnerin, J. P.; Edmondson, S. D.; Mastracchio, A.; Parmee, E. R.; Singh, S. B.; Becker, J. W.; Van der Ploeg, L. H.; Tota, M. R. *Biochemistry* **2004**, *43*, 6091.
- (a) Lee, M. E.; Markowitz, J.; Lee, J. O.; Lee, H. *FEBS Lett.* **2002**, *530*, 53; (b) Card, G.; England, B.; Suzuki, Y.; Fong, D.; Powell, B.; Lee, B.; Luu, C.; Tabriziad, M.; Gillette, S.; Ibrahim, P.; Artis, D.; Bollag, G.; Milburn, M.; Kim, S.; Schlessinger, J.; Zhang, K. *Structure* **2004**, *12*, 2233.
- Card, G. L.; England, B. P.; Suzuki, Y.; Fong, D.; Powell, B.; Lee, B.; Luu, C.; Tabriziad, M.; Gillette, S.; Ibrahim, P. N.; Artis, D. R.; Bollag, G.; Milburn, M. V.; Kim, S. H.; Schlessinger, J.; Zhang, K. Y. J. *Structure* **2004**, *12*, 2233.
- Zhang, K. Y. J.; Card, G. L.; Suzuki, Y.; Artis, D. R.; Fong, D.; Gillette, S.; Hsieh, D.; Neiman, J.; West, B. L.; Zhang, C.; Milburn, M. V.; Kim, S. H.; Schlessinger, J.; Bollag, G. *Mol. Cell* **2004**, *15*, 279.
- Kohno, Y.; Takita, S.; Ochiai, K.; Eiraku, T.; Kojima, A. *Jpn. Kokkai Tokkyo Koho*, 2008069144.
- Nishino, K.; Ohkubo, H.; Ohashi, M.; Hara, S.; Kito, J.; Irikura, T. *Jpn. J. Pharmacol.* **1983**, *33*, 267.
- Wilson, K.; Chissick, H.; Fowler, A. M.; Frearson, F. J.; Gittins, M.; Swinbourne, F. *J. Xenobiotica* **1991**, *21*, 1179.